X-613-68-430
PREPRINT

NASA TM X- 63402

ROCKET SPECTROGRAPHIC OBSERVATIONS OF α VIR

A. M. SMITH

NOVEMBER 1968

GODDARD SPACE FLIGHT CENTER
GREENBELT, MARYLAND

ROCKET SPECTROGRAPHIC OBSERVATIONS OF α VIR

by

Andrew M. Smith

Goddard Space Flight Center
National Aeronautics and Space Administration
Greenbelt, Maryland

Received:________________

ABSTRACT

Two spectrograms of α Vir (B1 V) in the wavelength interval $928<\lambda<1350$Å and with 0.8Å resolution were successfully recorded on a rocket flight June 1, 1967. The data revealed hydrogen Lyman absorption lines through L-ζ, and in addition, evidence for 128 absorption lines arising from the ground and low lying states in ions of C, N, Si, S, Cl, Ti, V, Cr, and Fe. An empirical flux distribution is derived from the data and compared to the fluxes of a model atmosphere for which Te = 22,600°K and in which the Lyman transitions are the only source of line absorption. The results imply that strong line blanketing occurs at $\lambda<1350$Å. No interstellar absorption lines due to H_2 were observed; an upper limit for the mean number density of this molecule between the earth and α Vir is $3.1 \times 10^{-4}cm^{-3}$.

INTRODUCTION

Rocket and satellite measurements of stellar fluxes have clearly shown a large flux deficiency in the far ultraviolet spectral region of main sequence B-type stars when compared to model atmospheres in which line absorption has been excluded. The photometric measurements of Chubb and Byram (1963); Smith (1967); and Stecher (1967) have illustrated this fact quantitatively. The spectrographic experiments of Morton and Spitzer (1966); Morton (1967); Carruthers (1968); and Morton, Jenkins, and Bohlin (1968) indicate strong ultraviolet line absorption and through the efforts of these workers and others many identifications of the more important lines have been made. The spectrographic results have so far extended down to λ1050Å, and in this paper shall be extended further to include the Lyman ζ line near λ930Å.

Gaustad and Spitzer (1961) have pointed out and discussed theoretically the many strong absorption lines in this wavelength region which can be expected. Accordingly, models in radiative equilibrium have been constructed for a B1.5 V atmosphere (Mihalas and Morton, 1965) and a B4 V atmosphere (Adams and Morton, 1968) including the effects of 98 ultraviolet absorption lines in the opacity. A similar model for a BO V star has been constructed (Hickok and Morton, 1968) using 104 ultraviolet lines. The results indicate a generally depressed flux level at $\lambda \lesssim 1300$Å for stars of this type. However, the predicted deficiencies do not yet seem to be as large as the observed deficiencies, and in particular it is not clear that sufficient account has been taken of the many weaker absorption lines which can be expected to contribute to the opacity.

This paper presents the results obtained from two spectrograms of α Vir (B1 V) recorded in the range $928 \leq \lambda \leq 1344$Å. Again, large absorption is observed at these wavelengths, and the purpose of the paper is to identify at least some of the absorbing agents, suggest the presence of others, and to estimate their total effect.

In the absence of any observed H_2 it is also possible to derive an upper limit to the amount of this molecule between earth and α Vir.

THE EXPERIMENT

The instrumental package consisted of a one element "stigmatic mounting" grating spectrograph, a pointing control system, and telemetry instrumentation required to monitor the payload status. The spectrograph, which is described elsewhere (Hochgraf 1966; Mostrom 1966), is shown diagrammatically in Figure 1. Starlight fell upon a platinum coated concave grating ruled at 1200 lines/mm. The grating itself defined the instrumental aperture to be 14 cm^2. A stigmatic image was formed on the grating normal at the focal plane for $\lambda \approx 1216$Å, but on either side of the grating normal the diffracted image became astigmatic thereby decreasing the speed of the system. A modest sacrifice in speed was found desirable, however, since the intentional introduction of some astigmatism provided better grain statistics as well as better resolution. The instrument was adjusted to give about 1/4Å resolution in 1134Å, and a nearly linear dispersion of 33.4Å mm^{-1} throughout the entire recorded spectrum. A mechanical collimator located in front of the grating limited the field of view in the plane of dispersion to $\pm 1/2^{\circ}$ at the half-power transmission points. Similarly, a slot close to the focal plane defined the field of view normal to the dispersion plane to be $\pm 1^{\circ}$.

The film used in the experiment was Kodak Pathe SC5 which in combination with the instrument exhibits a sensitivity curve as shown in Figure 2. The calibration was carried out at Lyman-α and except for the absolute value of the abscissa represents a characteristic curve for this type of film. Three calibrations using different strips of flight film were made in which the diffracted image of the slit source was shifted in 1Å increments over a small area of each strip. Under the assumption that there was no reciprocity failure (Fowler, Rense, and Simmons, 1965) the exposure time was varied with each position, and the source intensity was kept constant. Figure 2 shows the averaged results corresponding to an exposure of 150 sec. The development procedure used throughout the experiment included slight agitation of the exposed film for 2 minutes in D19B at 68^{o}F. The dashed portions of the curve indicate regions where the data are unreliable. The solid portion, derived from relatively reliable data, defines a very small dynamic range of a factor of 2. Relative flux values falling outside this range are extemely uncertain, consequently it is difficult to estimate the threshold sensitivity. There is evidence, however, that some sensitivity exists for flux levels a factor of 10 below that necessary to produce half maximum density in the film. In addition to the difficulty of a small dynamic range it has been observed that flux levels corresponding to half maximum density vary by as much as a factor of 2 for samples of film from the same batch; however, for a given sample this same flux level was observed to vary less than 10% in the wavelength range recorded, i.e. 928 $<\lambda<$ 1343Å.

The experiment package was launched at White Sands, N. Mex. at 2130 hrs (MST) on June 1, 1967 by an Aerobee 150 rocket. Based on the data of Struve, Sahade, Huang and Zebergs (1958) the relative radial velocity between the components of this binary system at the time of launch was 67 km sec^{-1}. Consequently, the wavelength difference between identical lines associated with each component is less than 0.3Å for all wavelengths in the present experiment. These same authors further suggest that the secondary component is type B7 in terms of its mass, but exhibits a spectrum of a B2 or B3 star because of its non-synchronous rotation and consequential heating of its entire surface by the primary component. In view of these facts no spectrographic discrimination between the two components was expected. During most of the flight when spectrograms were being recorded the spectrograph pointed at the star to within ± 10 seconds of arc, this being achieved by the "STRAP II" pointing control system developed at the Goddard Space Flight Center. Two exposures were taken, one at a mean altitude of 164 km for 150 sec, and the other at 127 km for 54 sec. The payload was recovered and the film subsequently developed according to the calibration procedures. The wavelength scale was determined by fitting the easily identified features of Lyman-α, Lyman-δ, and NII (λ1085.1Å) to a quadratic function of the distance measured on the film along the spectrum from an arbitrary starting point. The scale is believed to be accurate to within 0.3Å. The resolution was approximately 0.8Å limited mainly by the rocket motion.

THE RESULTS

Figure 3 is an enlarged reproduction of both spectrograms with the strongest lines identified. Figure 4 presents in 3 wavelength sections microdensitometer traces which have been smoothed in a computer using a triangular weighting function 0.62Å full width a half maximum. The lower and upper traces in each section correspond to the long and short exposures respectively. Vertical lines corresponding to laboratory-measured transitions indicate various spectral features which are definitely or possibly present. The horizontal lines connect members of the same multiplet, but for purposes of clarity all such members are not necessarily shown.

The fluctuations within the resolution element of 0.8Å are commensurate with the expected photon statistics. Examination of the flight film, however, indicates that grain noise must also contribute to the fluctuations, and that the data quality could have been improved by elongating the image normal to the dispersion plane without a significant loss in sensitivity.

Both spectrograms exhibit strong telluric line absorption. Features due to N_2 at λ960.2 and 965.6Å are the most obvious while absorption at λ972.1 and 977.0Å is expected to be even greater on the basis of laboratory data (Watanabe, 1961). These latter transitions occur in the same region where strong stellar absorption due to CIII and HI is expected, irrevocably confusing the observations at these wavelengths. The positions of other N_2 transitions are shown, and are perhaps reflected in the data; note for example, features at λ942.4 and 946.1Å.

The only obvious evidence for telluric O_2 is on the short exposure (mean altitude of 127 km) at λ1244Å. A weak feature corresponding to this wavelength can also be seen on the long exposure. As determined from the Cospar International Reference Atmosphere (1965) and the cross section measurements of Watanabe (1961) transitions at λ966, 972 and 983Å can be expected to be about the same strength or less. Transitions at λ939, 948 and 956Å may be as much as 6% stronger, but absorption by N_2 probably predominates at these wavelengths. A transition in O_2 at λ1205Å is suggested in both traces, but it has small effect indeed on the strong SiIII blend at λ1206.5Å. Except in the absorption bands noted, the N_2 and O_2 molecules above these rocket altitudes should have negligible effect on the stellar spectrum.

On the short exposure OI may produce a weak feature at λ1306Å, and probably contributes to the width of the Si III lines observed at λ1301.2 and 1303.3Å. The OI absorption is considered telluric, particularly in view of the fact that no interstellar lines can be definitely identified in these spectra.

No emission features have been detected. The peak near λ1110Å on the long exposure is a film blemish, and can be located on the corresponding spectrum reproduction in Figure 3.

Morton (1965) has listed 24 multiplets with lines expected to be wider than 2Å in stars of this type and in the wavelength range 928<λ< 1350Å. Lines in all of these multiplets have been identified with the exception of an Ar II transition at λ932.05Å. The latter is probably blended with the Lyman-ζ line to such a degree that it cannot be detected. Apart from the strong expected lines a number of tentative identifications have been attempted. For example, as expected the C II doublets near λ1335 and 1037Å which include resonance transitions are clearly seen. There is also, however, evidence for transitions in this ion starting from the 5.31 volt and 9.25 volt levels corresponding to features near λ1010Å in the first case and both λ1066 and 1324Å in the second.

Si II appears to be a stronger absorber at $\lambda 1193\text{Å}$ than S III. If this is the case one might expect to see the effects of Si II at longer wavelengths. There is indeed weak evidence on the short exposure for Si II multiplets near $\lambda 1265$, and 1309Å.

It may be noted here that none of the sulfur lines appear to be strong when compared, for example, with resonant absorption from Fe III at $\lambda 1122\text{Å}$. The strongest absorption feature due to sulfur is apparently a blend of S III lines near $\lambda 1201\text{Å}$. There also seems to be weak evidence for S II at $\lambda 1259.5$, 1253.8 and 1250.5Å which are resonant transitions of this ion.

Cl III appears as expected at $\lambda 1015$, 1009, and 1005Å but the Cl II lines at $\lambda 1071$, 1072, 1063, and 1079 are difficult to distinguish being blended with other features and particularly with the S IV lines at $\lambda 1074$, 1073 and 1063A.

Two Fe III multiplets are indicated here also. The lower levels in these transitions are near 3.1 ev, and the presence of their lines in the spectrum is uncertain. Perhaps the strongest evidence for absorption due to Fe III ions of low excitation may be found where two mutliplets are noted, one at $\lambda 1017\text{Å}$, and another at $\lambda 985.8$, 983.9 and 981.4Å. If this identification is accepted as plausible one might expect to find other features due to excited Fe III ions. Accordingly, such transitions have been noted throughout the range from $\lambda 980$ to 1150Å where they could possibly account for some of the observed structure. Attention is called to the region around the C II lines at $\lambda 1037\text{Å}$ where some of the features have been attributed to transitions from the ground state term of Cr III. Excited Fe III ions may also contribute to absorption in this region.

The spectrum possesses features probably arising in transitions from the ground state of the Fe II ion. The multiplet noted in the vicinity of $\lambda 1100\text{Å}$ indicates evidence to this effect. Again other Fe II ground state transitions which possibly are associated with spectral features are noted. Thus, the contour of the spectrum from $\lambda 1133$ to 1155Å may be principally influenced by the Fe II ion. Also there is some evidence on the short exposure that Fe II accounts for some of the features near λ1270Å.

In the category of possible low abundance elements the Cr III identification is the most certain. Three multiplets in the interval from λ1027Å to 1042Å provide the only observable transitions in the sensitivity range of the experiment, and it is considered quite likely that the features in this region are due in part to the Cr III ion.

Not so certain is the identification of ground state transitions in Ti III near λ1290Å. Some lines would be masked by those of the more abundant Si III ions; others may be associated with weak spectral features particularly at λ1286.4 and 1291.[illegible]Å.

Finally, an attempt was made to identify ground state transitions of V III with structure observed near λ1165Å. The correlation, however, is weak. Another multiplet of V III which might contribute to absorption centers around λ1152Å, and if significant would combine its effect with that of Fe II. The strong absorption associated with the ground state of Fe III would completely predominate at λ1123Å where another V III ground state multiplet is found.

There is much structure in the spectrograms which is not accounted for. An absorption feature at λ1230Å is revealed on the short exposure which may be telluric in view of the fact that it is not well reproduced in the long exposure. Absorption lines near λ1327, 1316, 1211, 1183 and 1117Å seem real but unidentifiable. A line near λ1137Å may be an unclassified line of Cr III at λ1136.67Å. There is a depression on either side of the C III line at λ1175.1Å which extends for several Angstroms and a general decrease in density with decreasing wavelength in a region just above the N II lines at λ1085Å. No agents accountable for these effects could be identified. The same may be said for the region near λ1053Å where the λ1055.27Å line of Fe II is considered only a possible identification, and the line at λ1054.4Å does not correspond well to any produced by H_2.

Table I contains a list of all multiplets in which at least one transition has been identified in the tracings. The ion species appear in column 1, the laboratory and observed transition wavelengths in columns 2 and 3 respectively, and the multiplet number in column 4. All the information contained in columns 1, 2 and 4, is taken from An Ultraviolet Multiplet Table of Moore (1950) except in the case of silicon where her Selected Tables of Atomic Spectra (1965) was used. Listed in column 5 are gf-values as compiled by Morton (1965), Wiese, Smith and Glennon (1966), or Garstang and Shamey (1967). In column 6 are comments which include crude estimates of the observed stellar line intensities ranging from very strong to very weak in five steps. For a weak or very weak classification the certainty of the identification is also given as either probable or possible. Blends of lines in the same multiplet are indicated where applicable.

DISCUSSION

The data indicate that not only are the strong lines employed by Mihalas and Morton in their B1.5 V model present in the atmosphere of α Vir, but that many other weaker lines appear as well. These arise in transitions from low lying levels in both abundant ions, e.g., Fe III, and less abundant ions, e.g., Si II, Fe II, Cr III, Ti III, and V III. Only for the ions of Fe II and Fe III have transitions been noted originating from levels not included in the ground state configurations. It is not unreasonable to expect, however, that similar transitions will occur in the other observed metallic ions and perhaps in some which remain unobserved such as Mn III or Mn II within the experimental wavelength range. Thus, in the atmosphere of α Vir the line blanketing due to weak but numerous lines is indeed significant, and may be comparable in strength to the opacity of continuous absorption sources.

If such a situation prevails, the wings of the hydrogen Lyman lines will be unobservable and, therefore, the measured line profiles will not provide a suitable comparison with Stark broadened lines derived theoretically. The cores of the

Lyman lines remain of course, but since these are formed high in the stellar atmosphere the theory is inadequate for comparison with the data. In any event it would be difficult to correct the profiles for the effe : of interstellar hydrogen without a reliable independent measurement of the interstellar hydrogen abundance. If it is assumed, for example that the mean number density of atomic hydrogen between the earth and α Vir is 0.1 cm^{-3} then the width of the observed Lyman-α line at half minimum is widened by a factor of about 1.14.

Spitzer, Dressler, and Upson, II (1964) have listed a number of lines in the Lyman bands of H_2 corresponding to transitions from v = 0 of (X) $^1\Sigma g^+$ to v' = 0, 1, ...13 of (B) $^1\Sigma_u^+$ with J = 0 and 1. Some of their data for lines which could possibly be detected among the observed stellar lines of α Vir are reproduced in Table 2.

The first and second columns contain the vibrational quantum numbers of the lower and upper states, the third column the Franck-Condon factors, and the fourth, fifth and sixth columns contain the only possible lines for transitions from the J = 0 and 1 rotational levels of the ground state. The positions of these lines are indicated in Figure 4 and are referenced by the vibrational quantum numbers in column 2. For the strongest vibration transition (v' = 4) the spectrogram contains no convincing evidence for any of the possible lines. Some features are observed near the lines for which v' = 1, 2, 8 and 13, but with the exception of the v' = 1 transition the correlation between the apparent absorption features and the actual line positions is weak. Furthermore, these vibrational transitions are relatively weak, and would not be expected if the v' = 4 transition were not observed. The average equivalent width of all the small apparent absorption features for each of the listed v' is 0.053Å. The RMS equivalent width of clear plate noise is 0.040Å which represents an optimistic limit of detectability. The absence of lines near λ1050Å together with the small average equivalent width, when compared to clear plate noise, of features at wavelengths corresponding to the listed electronic transitions argues against the detection of H_2 in this experiment.

A somewhat arbitrary condition for an identification of H_2 is that there should be correlation between the lines of the 0-2, 0-4, 0-7 and 0-8 vibrational transitions and observed features with equivalent widths greater than about 0.08Å. For the R(0) line in the 0-4 vibrational transition this figure corresponds to an upper limit of 6.5×10^{16} H_2 molecules cm^{-2} in the line of sight according to the calculations of Spitzer, Dressler, and Upson, II. The equivalent mean number density of 3.1×10^{-4} H_2 molecules cm^{-3} may be compared to the value estimated by Stecher and Williams (1967) for the general interstellar medium of $\sim 10^{-7} cm^{-3}$.

ACKNOWLEDGEMENTS

The initial concept and design of the rocket spectrograph was due to Mr. T. P. Stecher, whereas the final optical and mechanical designs were carried out by the Institute of Optics at the University of Rochester. I am indebted to many people in the Sounding Rocket Branch of this laboratory, in particular Messrs. S. B. Blanchard and R. M. Windsor, for their efforts to assure a successful performance of the telemetry and attitude control systems. I wish also to thank Mr. J. L. Shannon for the design and construction of the electronic control circuits associated with the spectrograph. Finally, I wish to thank Dr. D. A. Klinglesmith for use of several indispensible computer programs, and Mr. T. P. Stecher for many informative discussions.

REFERENCES

Adams, T. F., and Morton, D. C. 1968, Ap. J., 152, 195.

Carruthers, G. R. 1968, Ap. J., 151, 269.

Chandrasekhar, S. 1960, Radiative Transfer (New York: Dover Publications, Inc.).

Chubb, T. A., and Byram, E. T. 1963, Ap. J., 138, 617.

Cospar International Reference Atmosphere 1965 (Amsterdam: North-Holland Publishing Co.).

Fowler, W. K., Rense, W. A., and Simmons, W. R. 1965, Appl. Opt., 4, 1596.

Garstang, R. H., and Shamey, L. J. 1967, in The Magnetic And Related Stars, ed. R. C. Cameron (Baltimore: Mono Book Corp.)

Gaustad, J. E., and Spitzer, L. S., 1961, Ap. J., 134, 771.

Hickok, F. R., and Morton, D. C. 1968, Ap. J., 152, 203.

Hochgraf, N. A. 1966, J. Opt. Soc. Am., 56, 1418.

Mihalas, D. M., and Morton, D. C. 1965, Ap. J., 142, 253.

Moore, C. E. 1950, N.B.S. Circ., No. 488, Sec. 1

Moore, C. E. 1965, N.S.R.D.S.-N.B.S. 3, Sec. 1.

Morton, D. C. 1965, Ap. J., 141, 73.

Morton, D. C. 1967, Ap. J., 147, 1017.

Morton, D. C., and Admas, T. F. 1968, Ap. J., 151, 611.

Morton, D. C., Jenkins, E. B., and Bohlin, R. C. 1968, preprint Princeton University.

Morton, D. C., and Spitzer, L. 1966, Ap. J., 144, 1.

Mostrom, R. M. 1966, unpublished Ph.D. thesis, University of Rochester.

Spitzer, L., Dressler, K., and Upson, W. L., II. 1964, Pub. A.S.P., 76, 387.

Stecher, T. 1967, A. J., 72, 831.

Stecher, T. P., and Williams, D. A. 1967, Ap. J., 149, L29.

Struve, O., Sahade, J., Huang, S. S., and Zebergs, V. 1958, Ap. J., 128, 310.

Watanabe, K. 1961, Contribution of the Hawaii Institute of Geophysics, No. 29.

Wiese, W. L., Smith, M. W., and Glennon, B. M. 1966, N.S.R.D.S.-N.B.S. 4, 1.

Table 1

INDICATED TRANSITIONS IN THE ULTRAVIOLET SPECTRUM OF α VIR

Ion	λ(Å) (Laboratory)	λ(Å) (Measured)	Multiplet No.	gf	Remarks
H I	1215.67	1215.8	UV(1)	0.8324	Very strong;
	1025.72	1025.7	UV(2)	0.1582	Lyman lines
	972.54	---	UV(3)	0.05798	
	949.74	949.5	UV(4)	0.02788	
	937.80	937.6	UV(5)	0.01560	
	930.75	930.2	UV(6)	0.009628	
C II	1335.71 } 1335.68 }	1335.7	UV(1)	1.60 0.11	Strong; blended
	1334.52	1334.4		0.52	
C II	1323.92	1323.9	UV(11)	2.30	Weak; probable iden.
C II	1066.12 } 1065.88 }	1066.0	UV(12)	0.28 0.49	Weak; probable iden; blended
C II	1037.02 } 1036.33 }	1036.6	UV(2)	0.24 0.12	Moderate; blended
C II	1010.37 1010.07 1009.85	1010.0	UV(7)	1.02 0.68 0.34	Weak; probable iden; blended
C III	1247.37	1247.8	UV(9)	0.27	Moderate
C III	1176.35 } 1175.97 } 1175.70 } 1175.57 } 1175.25 } 1174.92 }	1175.7	UV(4)	0.32 0.26 1.00 0.20 0.26 0.33	Very strong; blended
C III	977.03	~ 997	UV(1)	0.81	Very strong
N II	1085.70 1085.54 1084.57 1084.57 1083.98	1084.5	UV(1)	0.70 0.12 0.39 0.13 0.17	Very strong; blended
N III	991.58 } 991.51 }	991.8	UV(1)	0.64 0.072	Strong; λ991.58 and 991.51Å are blended, λ989.79 is partially blended
	989.79	989.8		0.36	
Si II	1309.27 1304.37	1309.1 1304.2	UV(3)	0.57 0.21	Weak; possible iden.
Si II	1265.02 } 1264.73 }	1265.0	UV(4)	0.62 6.2	Weak; possible iden.
	1260.42	---		3.6	

Table 1 (Cont'd.)

Ion	λ (Å) (Laboratory)	λ (Å) (Measured)	Multiplet No.	gf	Remarks
Si II	1197.39	1197.5	UV(5)	1.03	Weak; probable iden.
	1194.50	---		5.1	
	1193.28	1193.3		2.0	
	1190.42	---		0.92	
Si III	1303.32	---	UV(4)	0.50	Moderate
	1301.15	1301.2		0.40	
	1298.96 } 1298.89 }	1298.8		1.80	
	1296.73	1296.9			
	1294.54	---			
Si III	1206.51	1206.6	UV(2)	1.68	Very strong
Si III	1113.23 } 1113.20 } 1113.17 }	1113.1	UV(5)	2.00	Moderate; λ1109.94 and 1108.37Å are blended
	1109.97 } 1109.94 }	1109.8		1.20	
	1108.37	1108.0		0.40	
Si III	997.39	997.3	UV(6)	1.00	Moderate
	994.79	994.7		0.64	
	993.52	---		0.20	
Si II	1259.53	1259.5	UV(1)	1.34	Weak; possible iden.
	1253.79	1254.2		0.89	
	1250.50	---		0.45	
S III	1202.10 } 1201.71 } 1200.97 }	1202.0	UV(1)	0.021 0.32 1.77	Weak; probable iden; λ1202.10, 1201.71 and 1200.97Å are blended; λ1194.40 and 1194.02Å are blended
	1194.40 } 1194.02 }	1194.1		0.32 0.94	
	1190.17	1190.2		0.42	
S III	1021.32 } 1021.10 }	1021.3	UV(2)	1.12 0.38	Weak; probable iden; λ1021.32 and 1021.10Å are blended; λ1015.76 and 1015.51Å are blended
	1015.76 } 1015.51 }	1015.7		0.38 0.52	
	1012.49	1012.3		0.30	
S IV	1073.52 } 1072.99 }	1073.1	UV(1)	1.69 0.19	Weak; probable iden; λ1073.52 and 1072.99Å are blended
	1062.67	1062.6		0.94	

Table 1 (Cont'd.)

Ion	λ (Å) (Laboratory)	λ (Å) (Measured)	Multiplet No.	gf	Remarks
Cl II	1079.08	1078.8	UV(1)	0.94	Very weak; possible
	1071.76	1072.0		0.56	iden; λ1071.76 and
	1071.05			2.82	1071.05Å are
	1063.83	1063.5		0.94	blended
Cl III	1015.02	1014.8	UV(1)	1.66	Weak; probable
	1008.78	1009.0		1.10	iden.
	1005.28	---		0.56	
Ti III	1298.67	---	UV(1)	---	Very weak;
	1298.95	---		---	possible iden.
	1295.91	---		---	
	1294.67	1293.7		---	
Ti III	1294.67	1293.7	UV(2)	---	Very weak;
	1293.26	---		---	possible iden.
	1291.64	1291.8		---	
	1289.32	1289.4		---	
	1286.38	---		---	
	1282.49	---		---	
V III	1169.28	1169.4	UV(1)	---	Very weak;
	1166.58	1166.2		---	possible iden.
	1166.47			---	
	1163.27	1162.7		---	
	1159.77	1159.8		---	
Cr III	1041.34	1040.9	UV(1)	---	Weak; probable
	1040.17	1040.1		---	iden; λ1040.17
	1040.05			---	and λ1040.05Å
	1037.80	1037.6		---	are blended
	1036.03	---		---	
	1035.93	---		---	
	1033.69	1033.8		---	
Cr III	1035.77	---	UV(2)	---	Weak; probable
	1035.57	---		---	iden; λ1033.99,
	1035.29	---		---	1033.69, 1033.45
	1033.99	---		---	and 1033.23Å are
	1033.69	1033.8		---	are blended
	1033.45			---	
	1033.23			---	
	1030.89	---		---	
	1030.47	1030.2		---	
Cr III	1030.10	1030.2	UV(3)	---	Weak; probable
	1029.57			---	iden; λ1030.10
	1028.33	1028.4		---	and 1029.57Å are
	1027.46	---		---	blended

Table 1 (Cont'd.)

Ion	λ (Å) (Laboratory)	λ (Å) (Measured)	Multiplet No.	gf	Remarks
Fe II	1275.80	1275.6	UV(9)	---	Very weak;
	1275.15			---	possible iden.
	1272.64			---	
	1272.00	1272.0		---	
	1271.24			---	
	1267.44	1266.8		---	
	1266.69			---	
	1260.54	---		---	
Fe II	1154.40	1154.3	UV(10)	---	Very weak;
	1153.96			---	possible iden.
	1153.28	---		---	
	1152.88	---		---	
	1152.44	---		---	
	1151.16	1151.1		---	
	1150.69	---		---	
	1150.29	---		---	
	1148.30	---		---	
	1147.41	1147.6		---	
	1146.96			---	
	1144.95	---		---	
	1143.24	---		---	
	1142.33	---		---	
Fe II	1142.33	---	UV(11)	---	Very weak;
	1138.64	1138.6		---	possible iden.
	1133.68	---		---	
Fe II	1104.98	1104.4	UV(18)	---	Very weak;
	1102.38	1102.3		---	possible iden.
	1101.54			---	
	1100.52	1099.9		---	
	1100.03			---	
	1099.12	1098.8		---	
	1096.89			---	
	1096.79	1096.4		---	
	1096.62			---	
Fe II	1062.76	---	UV(21)	---	Very weak;
	1059.57	---		---	possible iden.
	1055.27	1055.5		---	
Fe III	1131.91	1131.9	UV(1)	0.17	Moderate
	1131.19	1130.7		0.38	
	1130.40			0.50	
	1129.19			1.12	
	1128.72	1128.8		1.46	
	1128.02			1.17	
	1126.72	1127.0		0.88	
	1124.88	1125.3		2.32	
	1122.53	1122.5		4.50	

Table 1 (Cont'd.)

Ion	λ (Å) (Laboratory)	λ (Å) (Measured)	Multiplet No.	gf	Remarks
Fe III	1075.02	1074.9	UV(26)	---	Very weak; possible iden.
	1071.75	---		---	
	1066.18	---		---	
Fe III	1063.87	---	UV(40)	---	Very weak; possible iden.
	1061.71	1061.2		---	
	1061.24			---	
Fe III	1038.36	1038.4	UV(20)	---	Very weak; possible iden.
	1035.77	---		---	
	1032.12	1032.3		---	
Fe III	1033.30	---	UV(28)	---	Very weak; possible iden.
	1030.92	1031.2		---	
	1026.79	---		---	
Fe III	1024.11	---	UV(41)	---	Very weak; possible iden.
	1021.56	---		---	
	1019.79	1019.4		---	
Fe III	1018.29	---	UV(12)	---	Very weak; possible iden.
	1017.74	1017.8		---	
	1017.25	1017.2		---	
Fe III	999.38	999.4	UV(21)	---	Very weak; possible iden.
	997.60	---		---	
	995.15	---		---	
Fe III	985.82	985.8	UV(13)	---	Very weak; possible iden.
	983.88	983.3		---	
	981.37	981.4		---	

TABLE 2

VIBRATIONAL OSCILLATOR STRENGTHS AND WAVELENGTHS FOR THE LYMAN BANDS OF H_2

v	v'	VIBRATIONAL f_ν FACTOR	WAVELENGTH (Å) R(o)	R(1)	P(1)
0	1	0.0294	1092.196	1092.734	1094.053
0	2	0.0685	1077.140	1077.700	1078.927
0	4	0.143	1049.386	1049.960	1051.034
0	7	0.117	1012.814	1013.814	1014.328
0	8	0.0877	1001.824	1002.452	1003.297
0	13	0.0527	954.414	955.065	955.710

FIGURE CAPTIONS

FIGURE 1.

Simplified diagram of the rocket spectrograph. Essentially a Wadsworth mounting, a stigmatic image is formed on the grating normal near $\lambda 1216$Å. A slot near the focal plane defines a field of view normal to the dispersion plane of $\pm 1^{\circ}$. The effective grating area, i.e. the instrumental aperture, is 14 cm^2, and is ruled at 1200 lines/mm. The grating is platinum coated.

FIGURE 2.

A calibration function of the entire rocket spectrograph system at $\lambda 1216$Å. The curve represents an average of three calibrations corresponding to a 150 sec exposure using three samples of Kodak Pathe' SC5 flight film. Ordinate values represent film densities averaged over the area of the densitometer slit.

FIGURE 3.

Two spectrograms of α Vir (B1 V) secured with the stigmatic mounting rocket spectrograph. The exposure times of the top and bottom spectrograms were 54 sec and 150 sec respectively. Some identifications of the stronger features are shown in which the numbers represent an approximate average of wavelengths in Angstrom units at which known ionic transitions occur.

FIGURE 4.

Microdensitometer traces of the α Vir (B1 V) spectrograms. The horizontal scale is in Angstrom units, and the ordinates represent densities of the long (150 sec) exposure only. The top and bottom tracings were made from the short and long exposures respectively with an effective densitometer slit width of 0.62Å. Vertical lines indicate various spectral featuaes which are definitely or possibly present; horizontal lines connect members of the same multiplet.

FIGURE CAPTIONS (Cont'd)

FIGURE 5.

Plot of the flux from α Vir at the earth as a function of wavelength computed on the basis of the calibration curve of Figure 2. The solid line represents the measured values, and the dashed line represents a model for which T_e=22,600^oK and in which the Lyman transitions are the only source of line absorption. The model line widths are forced to fit the observed line widths at L α and L δ. It is likely that the vertical scale should be multiplied by a factor of 2.

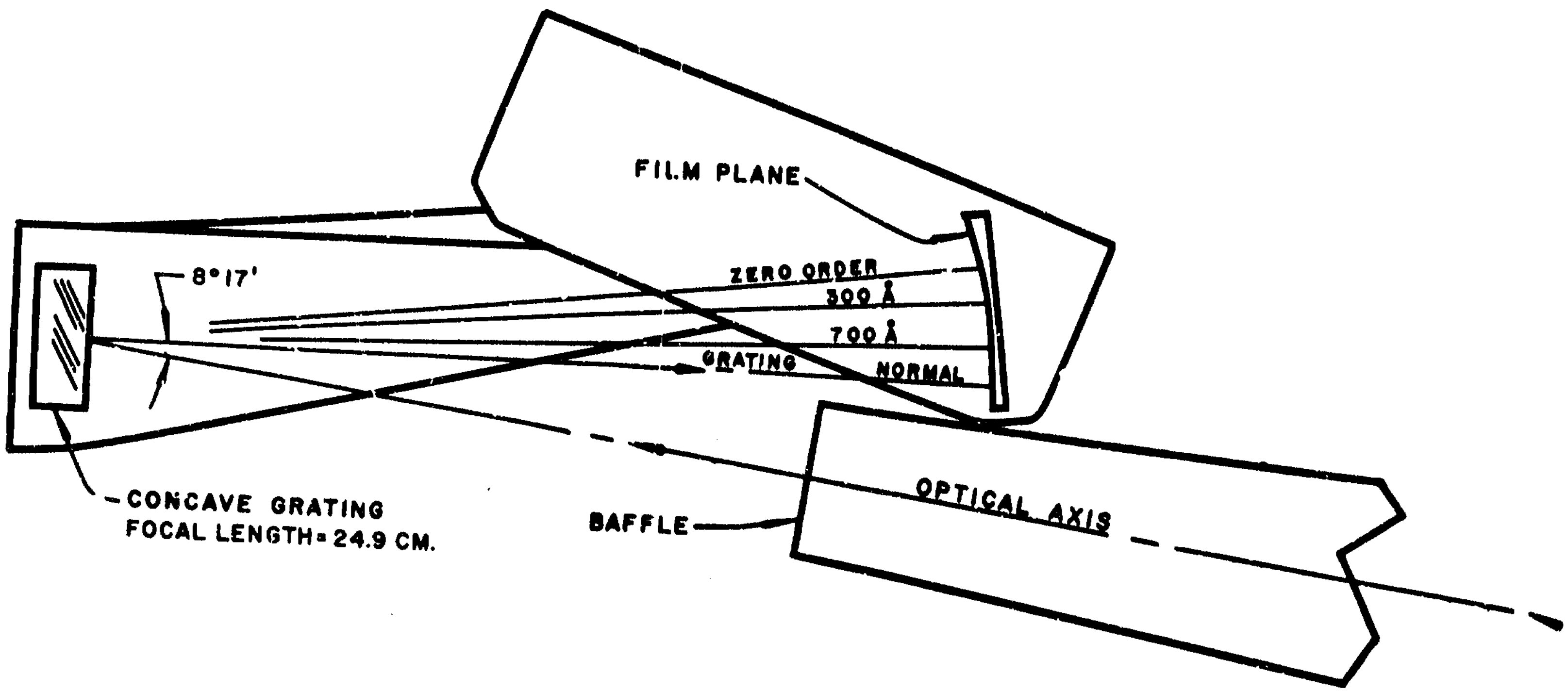
FILM PLANE
ZERO ORDER
300 Å
700 Å
GRATING
NORMAL
8° 17'
CONCAVE GRATING
FOCAL LENGTH = 24.9 CM.
BAFFLE
OPTICAL AXIS

FIG. 1

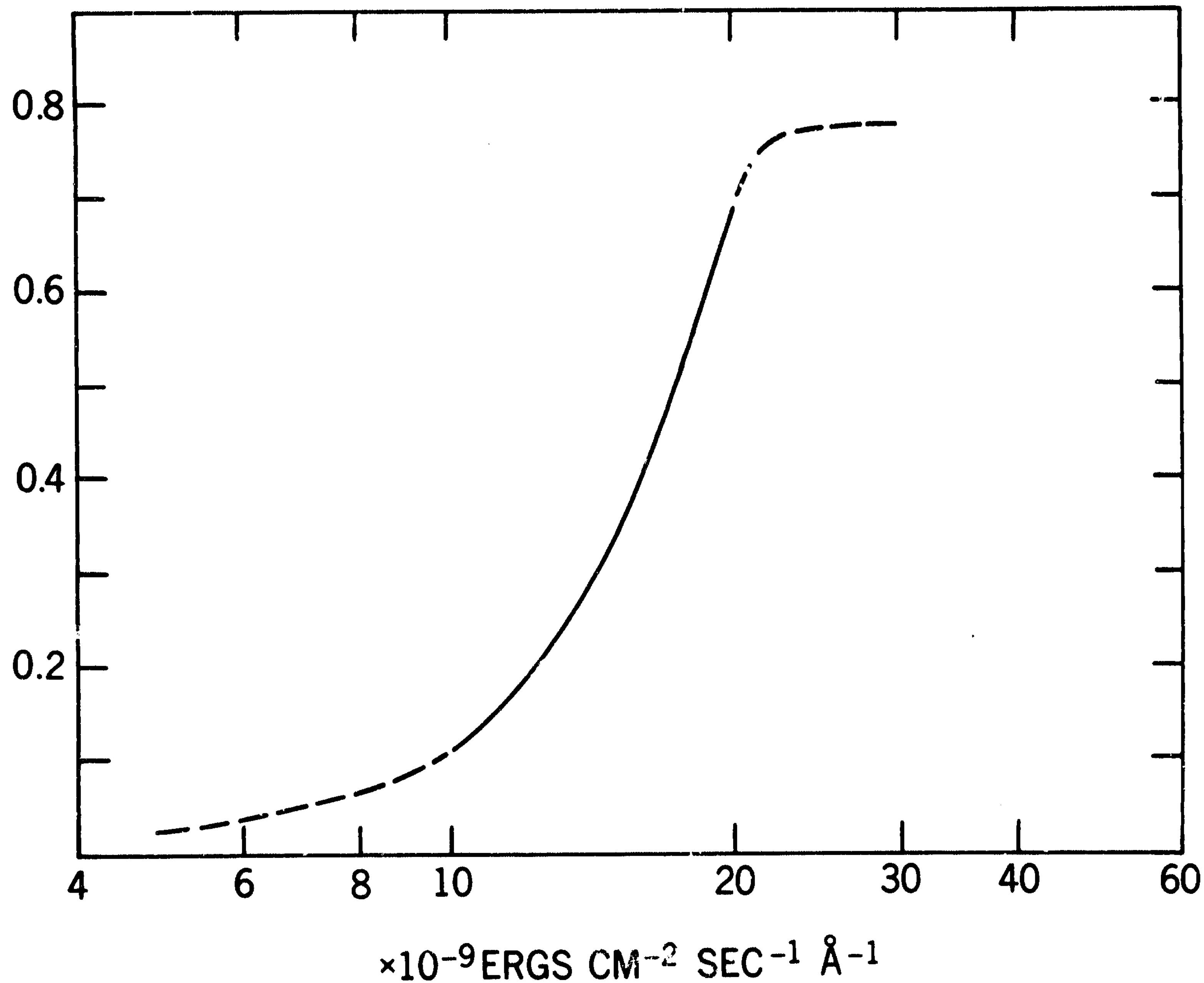

FIG. 2

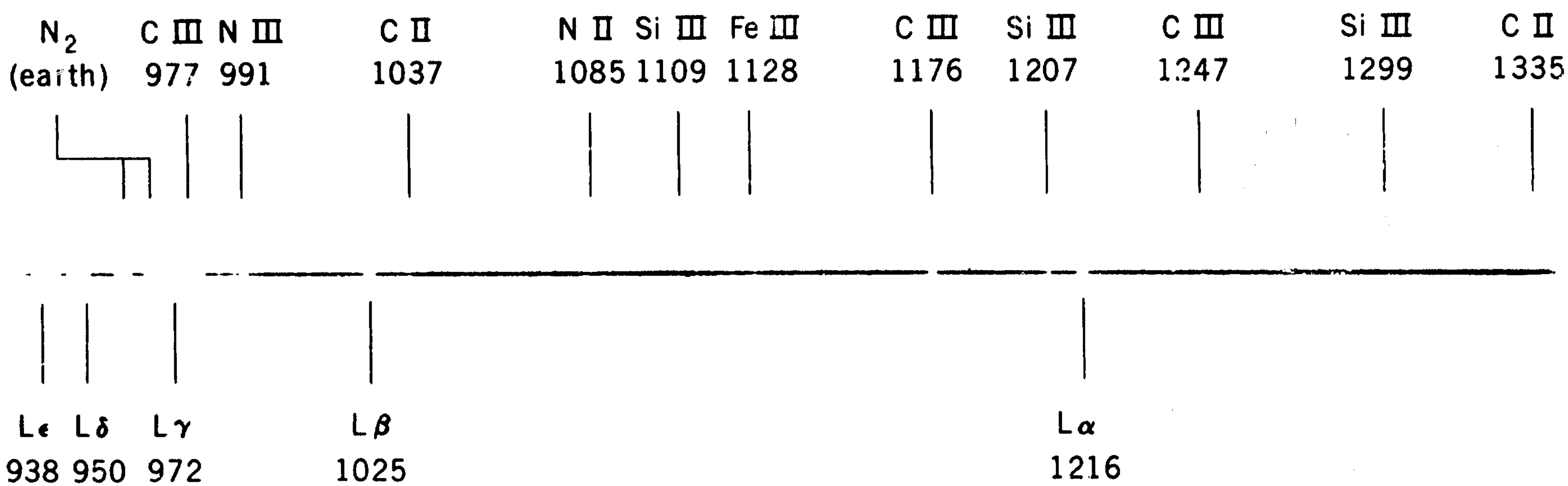

N_2 (earth)
C III 977
N III 991
C II 1037
N II 1085
Si III 1109
Fe III 1128
C III 1176
Si III 1207
C III 1247
Si III 1299
C II 1335
Lϵ 938
Lδ 950
Lγ 972
Lβ 1025
Lα 1216

FIG. 3

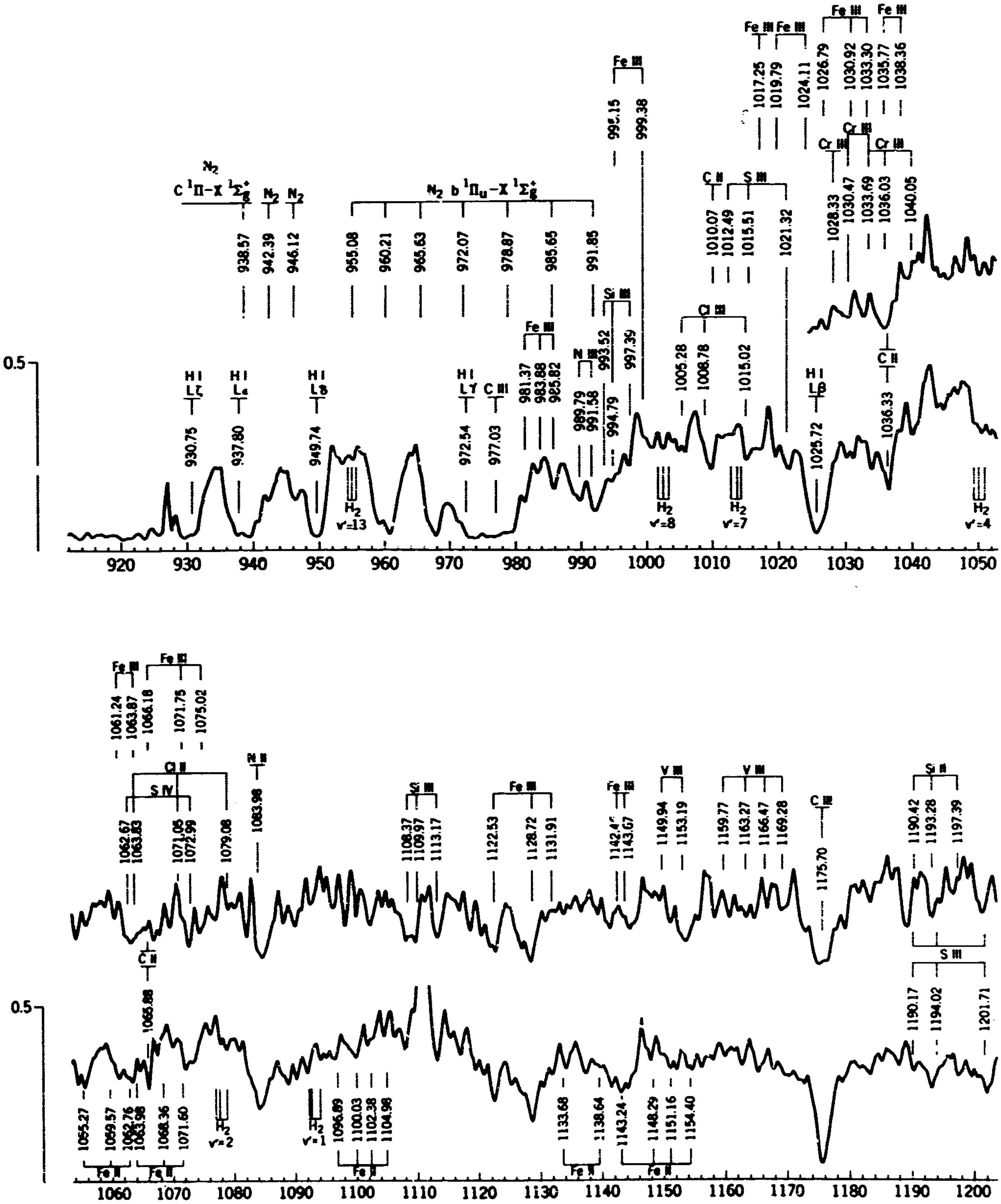

0.5
N_2 $C\,^1\Pi - X\,^1\Sigma_g^+$
938.57 942.39 946.12
N_2 N_2
N_2 $b\,^1\Pi_u - X\,^1\Sigma_g^+$
955.08 960.21 965.63 972.07 978.87 985.65 991.85
H I Lζ 930.75
H I Lε 937.80
H I Lδ 949.74
H I Lγ 972.54
C III 977.03
Fe III 981.37 983.88 985.82
N III 989.79 991.58
Si III 993.52 994.79 997.39
Fe III 995.15 999.38
Cl III 1005.28 1008.78 1015.02
C II 1010.07
S III 1012.49 1015.51 1021.32
Fe III 1017.25 1019.79 1024.11
Fe III 1026.79 1030.92 1033.30 1035.77 1038.36
Cr III 1028.33 1030.47 1033.69 1036.03 1040.05
H I Lβ 1025.72
C II 1036.33
H_2 v'=13
H_2 v'=8
H_2 v'=7
H_2 v'=4
920 930 940 950 960 970 980 990 1000 1010 1020 1030 1040 1050
Fe III 1061.24 1063.87 1066.18 1071.75 1075.02
Cl II 1062.67 1063.83 1071.05 1072.99 1079.08
S IV
N II 1083.98
Si III 1108.37 1109.97 1113.17
Fe III 1122.53 1128.72 1131.91
Fe III 1142.4 1143.67
V III 1149.94 1153.19
V III 1159.77 1163.27 1166.47 1169.28
C III 1175.70
Si II 1190.42 1193.28 1197.39
S III 1190.17 1194.02 1201.71
C II 1065.88
0.5
Fe II 1055.27 1059.57 1062.76 1063.98
Fe II 1068.36 1071.60
H_2 v'=2
H_2 v'=1
Fe II 1096.89 1100.03 1102.38 1104.98
Fe II 1133.68 1138.64
Fe II 1143.24 1148.29 1151.16 1154.40
1060 1070 1080 1090 1100 1110 1120 1130 1140 1150 1160 1170 1180 1190 1200

FIG. 4

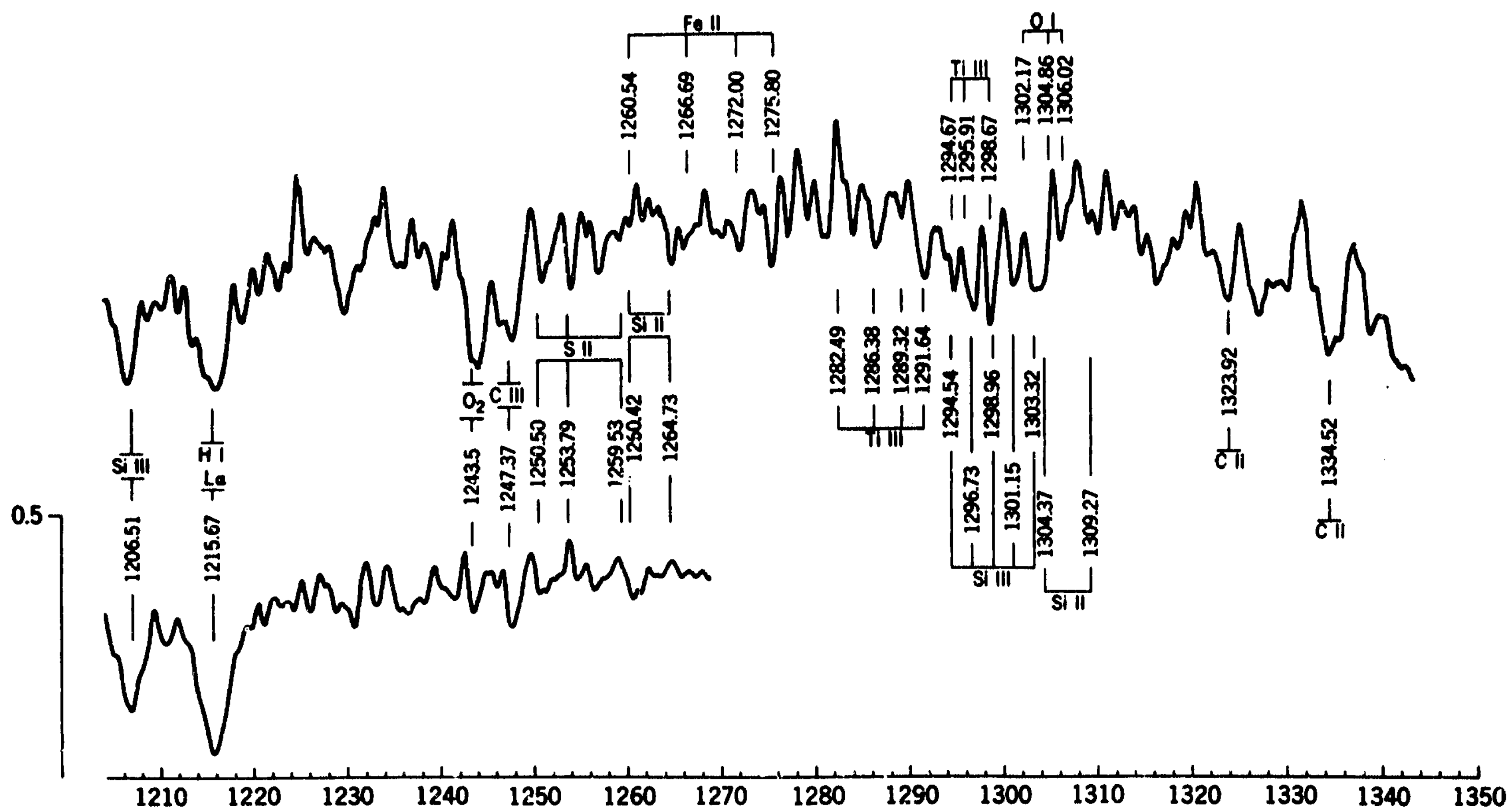

0.5
1206.51
Si III
1215.67
H I
La
1243.5
O2
1247.37
C III
1250.50
1253.79
1259.53
S II
1260.42
1264.73
Si II
1260.54
1266.69
1272.00
1275.80
Fe II
1282.49
1286.38
1289.32
1291.64
Ti III
1294.67
1295.91
1298.67
Ti III
1294.54
1296.73
1298.96
1301.15
1303.32
Si III
1304.37
1309.27
Si II
1302.17
1304.86
1306.02
O I
1323.92
C II
1334.52
C II
1210
1220
1230
1240
1250
1260
1270
1280
1290
1300
1310
1320
1330
1340
1350

FIG. 4 (CONT.)